Journal of the Physical Society of Japan
Vol. 65, No. 10, October, 1996, pp. 3186-3192

# A New Versatile Electron-Beam Ion Trap

Frederick John CURRELL, Junji ASADA, Koichi ISHII[1], Arimichi MINOH[2], Kenji MOTOHASHI[3], Nobuyuki NAKAMURA, Kazou NISHIZAWA, Shunsuke OHTANI, Kiyohiko OKAZAKI[2], Makoto SAKURAI[4], Hiroshi SHIRAISHI, Seiji TSURUBUCHI[3] and Hirofumi WATANABE

*University of Electro-Communications, Chofu, Tokyo 182*
[1]*Sumitomo Heavy Industries, Ltd. Niihama, Ehime 792*
[2]*Institute of Physical and Chemical Research (Riken), Wako, Saitama 351*
[3]*Tokyo University of Agriculture and Technology, Koganei, Tokyo 184*
[4]*Kobe University, Kobe, Hyogo 657*

(Received March 7, 1996)

We have constructed an electron-beam ion trap (EBIT) to facilitate the creation and study of highly charged ions. After a brief introduction to EBITs in general, we describe the design of the new device, highlighting its unique features. Some preliminary results are presented which demonstrate the devices capability to produce and study highly charged ions.

KEYWORDS: ion trap, EBIT, electron beam, trap, highly charged ions, X-ray source

## §1. Introduction

The first EBIT was constructed by Levine *et al.*[1)] to study the X-ray spectroscopy of highly charged ions. It was based on the earlier electron-beam ion source[2)] (EBIS) but with a shorter trap length to limit instabilities inside the trap and hence increase the residence time of ions. This increased residence time is the key to producing highly charged ions. For a number of years, two such devices have been in operation at Lawrence Livermore National Laboratory. More recently, similar devices have been constructed at Oxford,[3)] NIST[4)] and Tokyo.[5)] In this paper, we highlight the new features of the Tokyo EBIT and show some preliminary results.

The EBIT is well suited as a source for X-ray spectroscopy of highly-charged ions. The ions are at rest to a good approximation, having no centre-of-mass velocity so a Doppler correction does not need to be applied. The temperature of the ions depends on the specific trap configuration but for an ion of charge state $q$ it is typically less than $100q$ eV. Although several different charge states may be present at the same time it is possible to optimize the abundance of one particular charge state by choosing the trap conditions carefully. Interpretation of the resultant spectra is considerably simplified due to the negligible population of excited-state species in the trap (with the exception of rare metastable states with a lifetime in excess of 0.1 s) and the low density which removes any collisional or absorption effects.[6)] Since the ions in the trap form a weak-field plasma when compared to the field due to a highly charged ion's nucleus, Stark and magnetic field effects can usually be neglected.[6)] The magnetic field (typically 3 to 4.5 T) used in EBITs is negligible compared to the field produced locally in a highly charged ion due to a bound electron (typically 1000 T). The geometry of the trap is also ideal for X-ray spectroscopy. The X-ray source is defined by the electron beam, giving rise to a line source about 2 cm long with a 35 $\mu$m radius. This source can be used directly for dispersive spectroscopy without the need for an entrance slit. This is one particular benefit provided by the high magnetic field (compared to the field created by the space-charge of the electron beam at the cathode) at the trap region.

In addition to performing high-resolution X-ray spectroscopy studies of highly charged ions,[7)] EBITs have been used to study many other processes. For example, electron-ion collision processes such as dielectronic recombination,[8)] electron-impact excitation,[9)] resonant excitation,[10)] and ionization[11)] have been studied. More recently, ions extracted from an EBIT have been used in ion-surface interaction studies[12,13)] showing potential benefits in the field of surface modification. Extracted ions have also been retrapped to study ion-gas interactions.[14)]

A particularly noteworthy advance in the technology of EBITs was the upgrade of the original EBIT to be able to produce an electron beam up to 210 keV in energy.[15)] The higher energy "super-EBIT" was able to produce and study bare Uranium.[16)] Another significant advance was an injection technique which allows experiments to be performed with nanogram quantities of material.[17)] These advances make it possible in principle to use a super-EBIT to study any highly-charged ion of any isotope of any element with a lifetime greater than a few hours. Clearly the EBIT is a versatile device, capable of studying the physics of highly charged ions in many different ways. More details regarding the modes of operation, the types of experiments and the underlying technology can be found in a number of review articles.[18-20)]

In an EBIT, the electron beam is compressed and confined by a magnetic field. Typically, this field is generated by a pair of superconducting Helmholtz coils at liquid Helium temperature (4.2 K). The electron beam passes through a series of electrodes of cylindrical symmetry called drift tubes. Ions are trapped in the radial

direction by the space charge potential of the electron beam and the effective potential of the magnetic field. An axial electrostatic well is created by the application of appropriate voltages to the drift tube electrodes (i.e. the central drift tube has a negative potential with respect to the outer drift tubes). Ions are trapped for all positive charge-states, regardless of mass. The ions are created by successive electron impact ionization steps, starting from neutral gas or low charge-state ions introduced into the trap region. Each ionization event removes an electron, increasing the charge-state. This process continues until it is no-longer energetically possible (i.e. the next ionization potential is greater than the electron beam energy). Furthermore, the ionization cross-sections of highly charged ions tend to increase as the electron-energy increases above the threshold for ionization. Thus, the rate for production of highly-charged ions increases with increasing beam energy and current density.

The abundance of various charge states in the trap region is also determined by a number of other processes. Ions can capture electrons from the beam. The resultant excited state usually stabilizes by photon-emission, resulting in an ion of lower charge state. Charge exchange, between ions and background gas also acts to drive the charge balance towards lower charge states. This process does not change the net positive charge present in the trap since one species gains an electron as another loses one. The result of this process however is a reduction in the number of highly-charged ions since charge exchange predominantly occurs between highly charged ions and neutral species. To minimize the rate of this process, it is useful to obtain the lowest pressure possible in the trap region. Since the trap is surrounded by a liquid Helium vessel, the whole trap acts as an efficient cryo-pump which helps to create the high standard of vacuum required.

Coulomb interactions between the ions and the electron beam act to heat the ions. Eventually, the ions have enough energy to escape from the trap region. A technique called evaporative cooling[21] can be used to reduce the loss of high-Z ions through this mechanism. A carefully controlled amount of a low-Z gas (typically Neon) is introduced. Ions of the low-Z and high-Z species can easily exchange energy through Coulomb interactions. Since high-q, high-Z ions are trapped more efficiently than low-Z ions, the low-Z ions tend to escape from the trap. In so doing, they reduce the temperature of the high-Z ions (through the relatively fast coulomb interactions) and hence increase the residence time of high-Z ions.

All of the processes outlined above can be accounted for as an initial value boundary condition problem[22] to predict the behavior of an EBIT under various operating conditions. Solving this model involves the time evolution of a large set of coupled differential equations. Two equations are used for each charge-state of each species present in the trap, one representing the number density and one the temperature. Generally, the differential equations are stiff and require a small time-step during their solution.

Ions can capture electrons from the electron beam. The resultant excited state is usually stabilized by the emission of a photon. A portion of these photons can leave the trap at 90° to the electron beam and pass through the gap between the Helmholtz coils to a number of observation ports. Small apertures in the drift tube and the cryostats allow these photons to proceed unimpaired to the observation ports. Various spectrometers and detectors can be attached to these observation ports for optical spectroscopy. The total photon signal from the source is proportional to the product of the electron-beam current and the ion number density.

In summary, the desirable properties for an EBIT are high beam energy, high beam current, high magnetic field and good vacuum. These parameters in turn lead to high current density, high ion number density and access to high charge states.

## §2. The Device

A comparison of the relevant parameters for various EBITs, including the new Tokyo EBIT are given in Table I. The Oxford[3] and NIST[4] EBITs will have similar operational parameters to EBIT2 since they are of a very similar design. The Tokyo EBIT more closely resembles super-EBIT, with both the gun and the trap floating away from earth. When configured to operate at the maximum electron-beam energy, the whole trap region will float at +40 keV from earth (i.e. the main vacuum chamber wall). The gun will float at −300 keV from earth. Both the gun and collector are isolated from the main chamber by accelerator tubes. Inside the vacuum the insulation gaps were determined using an empirically based formulae[23] with a safety factor of about 2 in all cases. Electrical feedthroughs for the gun and collector systems come in through the top and bottom of the device respectively. In each case, the feedthrough is floated on the 300 keV main power supply. An overview of the Tokyo EBIT and its constituent parts is shown in Fig. 1.

Table I. A comparison of the operational parameters for different EBITs.

| Parameter | EBIT2† | Super-EBIT† | Tokyo-EBIT* |
|---|---|---|---|
| Beam Energy | 0.5–25 keV | 10–210 keV | 2.5–340 keV |
| Beam Current | 0–160 mA | 0–200 mA | 0–300 mA |
| Magnetic Field | 0–3 T | 0–3 T | 0–4.5 T |
| Electron Beam Radius | $\geq 35\,\mu$m | $\geq 35\,\mu$m | $\geq 35\,\mu$m |

†As given by Elliot.[18]
*Projected from a detailed design study.

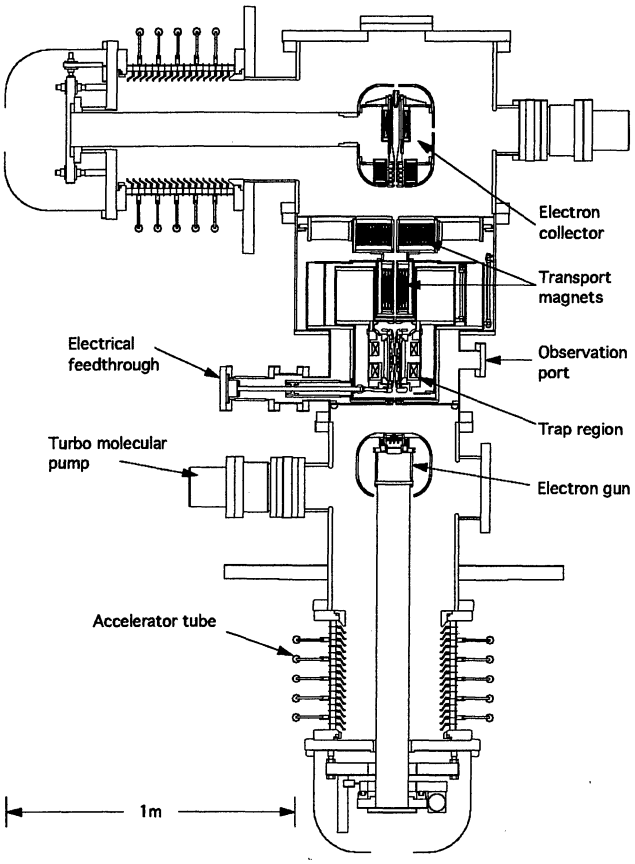


Fig. 1. A scale drawing showing an overview of the design of the Tokyo EBIT.

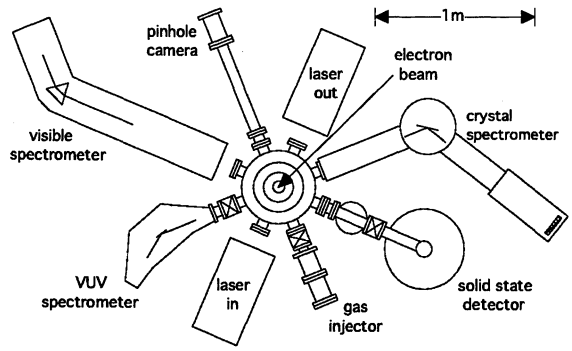


Fig. 2. A plan view of the use of various observation ports, including the spectrometer arrangement.

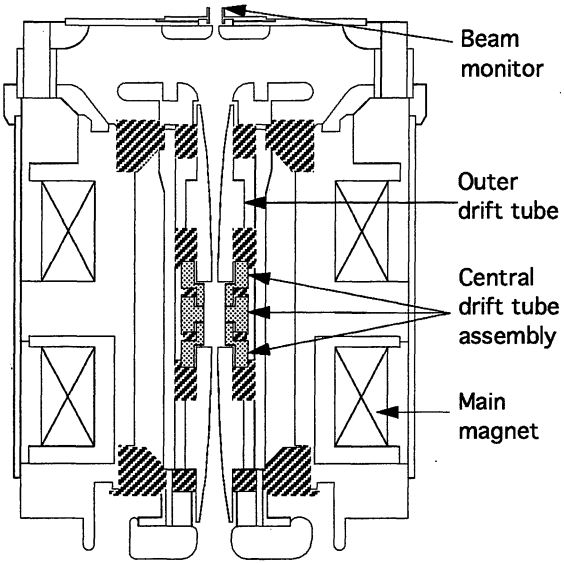


Fig. 3. Details of the design of the trap structure. Sapphire insulators are designated by the striped areas. The central drift tube assembly is dotted. This assembly is comprised of six insulated electrodes as described in the text.

### 2.1 *Observation ports*

A total of eight observation ports are situated around the trap to facilitate spectroscopy, beam diagnosis and gas injection. So far, only solid-state detectors have been used to study photons emitted from the trap region. A series of optical spectrometers are currently being constructed. The observation ports have been set up to accommodate the final experimental arrangement shown in Fig. 2. The apertures in the drift tubes and cryostat vessels which are used for X-ray measurements have been covered with thin Beryllium windows. These reduce the gas conductance from outside the cryostat region into the trap and hence improve the vacuum quality.

### 2.2 *Trap structure*

Since the whole design process (outlined below) implicitly assumed rotational symmetry, it is important to achieve the best possible alignment of the various components. Furthermore, misalignment may cause instabilities in the trapping of ions, limiting the charge states obtainable. The whole electron gun assembly can be translated or tilted in two orthogonal directions, perpendicular to the beam axis. The trap region can also be both translated and tilted in these same two directions. All of these adjustments can be made whilst the device is under vacuum. Using a travelling microscope, situated directly above the collector and looking down through an observation port it has been possible to align the gun, trap and collector axes with a precision of about 0.05 mm when the trap is at 4.2 K.

The trap structure is shown in detail in Fig. 3. In contrast to previous EBIT designs, the central drift tube has been split into 6 electrically insulated elements. Axially, the central drift tube has been split into three separate elements, the central one of which has been split into four sector elements. Hence when the electron beam is turned off, the trap becomes a cylindrical penning trap[24] capable of high precision charge to mass ratio and related measurements. Coherent ion motion has already been observed in an EBIT trap with a less suitable structure.[25] This new trap structure gives a choice regarding the type of ion motion induced and measured. Either cyclotron or axial motion studies can be performed. Furthermore, the extra electrodes give more freedom over the form of the electrostatic potential experienced by the trapped ions.

### 2.3 *The superconducting magnet and cryostatic region*

The superconducting magnet of the Tokyo EBIT routinely produces a 4.5 T magnetic field. It can be used in persistent current mode to remove power supply ripple.

During its construction, the magnetic field was measured and a small trim-coil was added to reduce the measured inhomogeneity. In this manner, a measured field inhomogeneity of less than $10^{-4}$ along the trap length of 3 cm has been obtained. This inhomogeneity is far worse than can be achieved by a single long solenoid but a Helmholtz coil arrangement is required to facilitate optical spectroscopy. Normally an EBIT's superconducting magnet and trap region are at 4.2 K. This temperature dictates the ultimate vacuum which can be achieved in the trap region and hence the trapping time of the highly charged ions. The Tokyo EBIT is the first device to overcome this limitation. The liquid helium entering the cryostat is overcooled, using the Joule-Thompson effect. In this manner, the EBIT has been run with the whole trap below 2.4 K. This temperature was determined by using two calibrated resistance thermometers (LakeShore Carbon-Glass Resistor model no. CGR-1-500) placed near the "warm holes" at the top and bottom of the trap region. The vapor pressure of Hydrogen decreases by more than 7 orders of magnitude[26] as the temperature falls from 4.2 K to 2.4 K. Since the pressure of the trap region should be dominated by the partial pressure of Hydrogen, a significantly improved vacuum should result from the overcooling.

### 2.4 *System diagnostics*

A novel series of beam-position monitors have been constructed which allow us to determine the position of the electron beam through the trap region in real time.[27] A small portion of the electron beam current is modulated by applying a square-wave switching the anode voltage between two levels. The change in the net charge in the beam capacitively couples to four electrodes in a square configuration. The difference signal on opposite pairs of electrodes then determines the positioning of the electron beam inbetween the electrodes. This diagnostic system monitors the location of the centre of charge (and hence the centre of gravity) of the electron beam. Two such systems are used, one before and one after the trap to monitor the beam trajectory through the trap region. These systems will be particularly beneficial when performing dispersive types of spectroscopy, comparing spectra taken under different operating conditions. Usually, when operating dispersive spectrometers with an EBIT, no entrance slit is used. Instead, the intrinsic width of the radiation source acts as a slit. The size of this source is the electron beam diameter. If the electron-beam position were to change due to a change in operating conditions, this would lead to a change in the energy-scale at the detector. Using the capacitive beam-position monitors, it will be possible to ensure this effect does not occur.

The design of one of these capacitive beam-monitors is shown in Fig. 4. The four sensor electrodes were positioned to shield the electron-beam from insulators. This positioning is necessary to prevent the insulators from charging up and causing electrical breakdown. One drawback with this arrangement is that the device no longer has mirror symmetry in the $X$ and $Y$ axes. Simulations show that this electrode arrangement has a slight

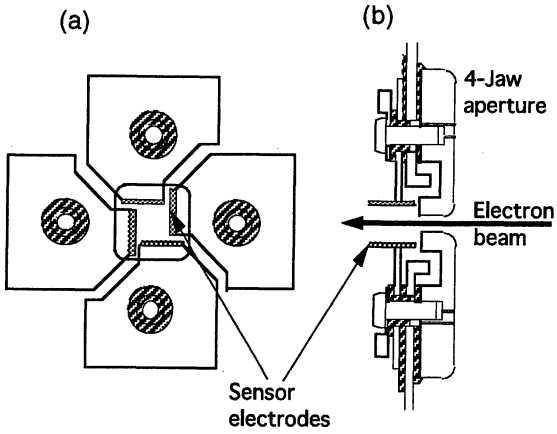


Fig. 4. The layout of one capacitive beam monitor used to measure the electron beam position. (a) shows the monitor end on (i.e. as seen from the electron gun). (b) shows the side view. Striped portions represent sapphire insulators. The dotted regions show the faces which sense the electron beam position.

coupling between the electron-beam's $X$ position and the monitors $Y$ signal and a similar coupling between the $Y$ position and the $X$ signal.[27] This coupling can be accurately calculated and then accounted for. In this application, the coupling is not a problem since we are interested in reproducing the beam position from run to run, rather than determining it on an absolute scale. It may also be possible to use the central sectored drift tube (Fig. 3) as a capacitive beam monitor although its geometry has been optimized to form an effective trap and to induce and study coherent ion motions.

A short distance before each capacitive beam monitor, there are 3 mm by 3 mm square apertures. Each aperture is composed of four insulated trapezium-shaped electrodes (four-jaw slits). The tails of the electron beam fall on these apertures, giving a further indication of the electron beam trajectory through the trap region and how well the device is tuned. A third similar four-jaw slit arrangement has been placed at the entrance to the collector assembly, again for diagnostic purposes when tuning the device.

Inside the trap region, at a distance of 25 mm from the central axis is positioned a 10 $\mu$m wide slit running parallel to the beam axis. This acts as a 1-dimensional pinhole camera. This slit is lined up with one of the observation ports. Using an X-ray sensitive imaging detector at this observation port, it is possible to determine the beam profile.

### 2.5 *Electron beam optics*

The electron beam comes from a pierce-type electron gun which comprises four electrodes of cylindrical symmetry. Electrons are emitted thermionically from a spherically-shaped Barium Oxide cathode of 3 mm diameter. The perveance of the gun is about $4.4 \times 10^{-6}$ A/V$^{3/2}$. In practice, the electron beam radius is not given by the Brillouin limit but by the radius predicted by Hermann theory.[28,29] This theory predicts the radius in which 80% of the electron beam is contained to be:

$$r_0 = r_b \left[ \frac{1}{2} + \frac{1}{2} \left\{ 1 + 4 \left( \frac{8kTr_c^2}{m\eta^2 r_b^4 B^2} + \frac{B_c^4 r_c^4}{B^2 r_b^4} \right) \right\}^{\frac{1}{2}} \right]^{\frac{1}{2}} \quad (1)$$

where $r_c$ is the cathode radius, $B_c$ the magnetic field at the cathode, $kT$ is the characteristic electron energy at the cathode, dictated by its temperature. $m$ is the electron mass and $\eta$ the electron's charge to mass ratio. Assuming the neutralization of the electron beam by the trapped ions to be small (in practice it is about 1%), the Brillouin radius $r_b$ is given in cm by:

$$r_b = \frac{0.015\sqrt{I_e}}{BE_e^{0.25}} \quad (2)$$

where $I_e$ is the beam current in $A$, $B$ is the magnetic field at the trap in Tesla and $E_e$ is the electron-beam energy at the trap, in keV.

From eq. (1) it is clear that to achieve maximum compression of the electron beam it is necessary to reduce the magnetic field at the cathode as much as possible (i.e. set $B_c$ to zero). To this end, the whole gun assembly is surrounded by soft iron which acts as a magnetic shield. Additionally, a solenoid (bucking coil) is used to cancel the residual field from the main magnet. The magnetic field distribution both inside and outside the soft iron shield was simulated using the Poisson/Superfish programs.[30] With the resultant magnetic field distributions, electron trajectories in the region of the electron gun were simulated using EGUN.[31] In practice, the bucking coil is adjusted along with other electron-gun parameters to optimize the operation of the device.

Further EGUN calculations were used to match the electron beam to the gradient of the magnetic field due to the superconducting solenoid and to study the electron trajectories near the collector. These calculations provide an initial set of parameters with which the EBIT can successfully be operated. In practice, several of the potentials and magnetic fields were usually adjusted to optimize the devices performance.

### *2.6 Power supplies and computer control*

Outside of the vacuum system, the 300 keV power supply, several power supplies which float on the 300 keV supply, control electronics, cabling and interconnections are all housed in a separate $SF_6$ tank. This housing system is designed to decrease the break-down gap required for high-voltage operation and hence prevent accidents during experiments operating at high energy. Briefly, each separate power-supply is programmed by a Digital to Analog Converter (DAC). Each DAC is controlled by a local microprocessor. In some cases, Analog to Digital Converters (ADCs) are used by the same local processor to read outputs of the power-supplies which are proportional to the voltage and current being supplied. The operator can control all the power-supplies from a single personal computer. This control computer communicates with the local processors via a fiber-optic network. The local processors can also store tables of values. These values can be successively written to one or more DACs simultaneously to generate time dependent waveforms as required.

The user interacts with the power-supplies through a graphically based object-oriented interface with each power-supply being treated as an object. Through the interface, the operator can set and read the output status of a power-supply (i.e. voltages and currents). In addition, any object representing a power supply may be connected to a number of "processes" which the software is continually performing. For example, it is possible to log the long-term behavior of a power-supply and thereby monitor any changes in the EBIT's operating conditions. This is achieved through the graphical interface by connecting the appropriate object to a process which sequentially updates a graph of a time series. A polling algorithm which is optimized to minimize network traffic between the host processor and the local processors is used to continually update the information being given to the various processes by the objects.

## §3. Results and Discussion

During the initial phase of operation of the EBIT, the device has been conditioned to run at gradually higher beam energies and currents. The highest electron beam energy was 80 keV and the highest current transmitted from the gun to the collector was 140 mA. It is anticipated that these parameters will continue to increase as the device becomes conditioned for high-Voltage operation. We have been able to get more than 99% of the emitted current to be absorbed by the collector over a wide range of operational parameters.

A typical X-ray spectrum measured with a Si(Li) solid state detector is shown in Fig. 5. The designations used for this spectrum are based on studies of other neon like ions.[32] We can see clear evidence for the creation and trapping of $W^{64+}$ at 20 keV beam energy with a transmitted electron current of 100 mA. No Tungsten is being injected from outside the vacuum chamber. Instead, the Tungsten is either sputtered or evaporated from the cathode. It then travels along the beam axis to eventually become trapped in the drift tube region. At low X-ray energy some structure is observed which may be due to neon-like Barium ions, also originating from the cathode. The highest energy radiative recombination peak pro-

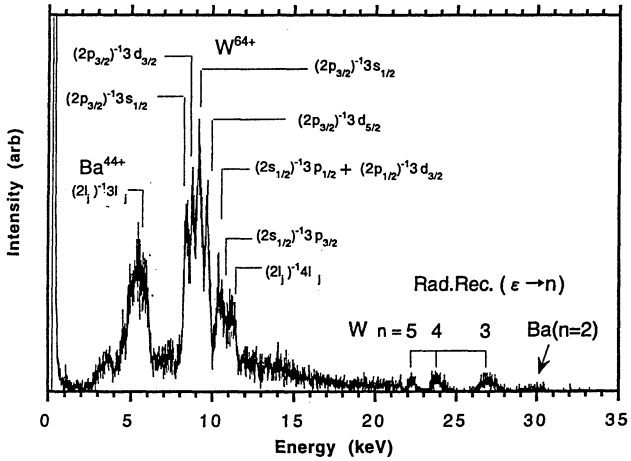


Fig. 5. An X-ray spectrum of $W^{64+}$ (neon like) taken using the Tokyo EBIT. Details are given in the main text.

vides further evidence for the trapping of Barium ions.

This spectrum has the general form expected, with a cluster of peaks about 10 keV due to electron impact excitation (IE) which are sitting on a slowly varying background due to bremsstrahlung radiation. The bremsstrahlung radiation continues up to the electron beam energy. Above the beam energy, three peaks are seen due to radiative recombination (RR) into the $n = 3$ to $n = 5$ shells. We made a small change to the electron beam energy (lowering it to 19 keV). Following this change to the operating conditions, the IE-peaks occurred at the same X-ray energy whilst the energy of the RR-peaks decreased by 1 keV. This is the expected energy dependence.

In addition to facilitating ion-motion experiments, the trap structure of the Tokyo EBIT gives greater flexibility in determining the form of the electrostatic potential in the trap region. A different electrostatic potential leads to different escape rates and affects the charge distribution. To investigate this effect, we performed X-ray measurements using the EBIT with different electrostatic settings under otherwise similar conditions. Two X-ray spectra taken when Krypton gas was being injected are shown in Fig. 6. During collection of the data shown in Fig. 6(a), the trap was configured so that the two "penning-electrodes" were at the same potential as the outer drift tubes. In this configuration, the axial potential distribution follows an inverted bell-shaped form, as shown in the insert to Fig. 6(a). Figure 6(b) shows a spectrum obtained using the usual almost square-shaped axial potential distribution.

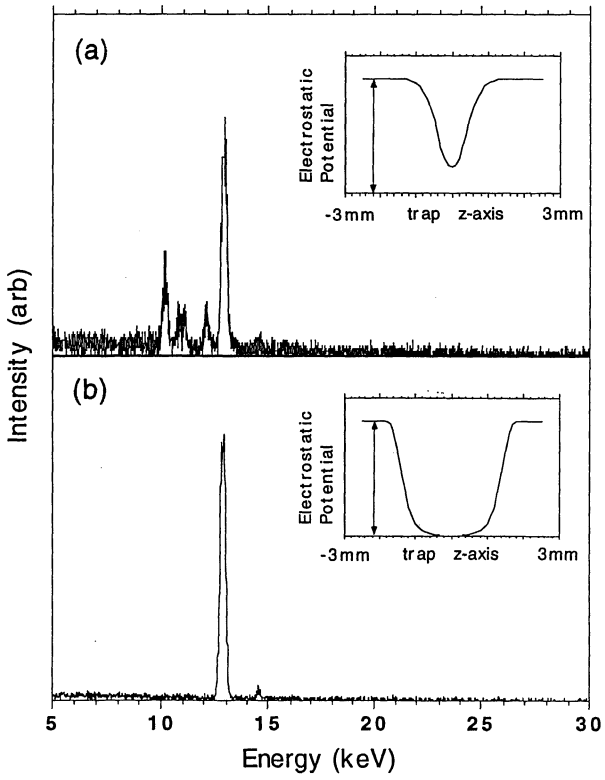


Fig. 6. A comparison of two X-ray spectra taken at 50 keV beam energy and 100 mA beam current, with neutral Krypton being injected into the trap. The form of the axial electrostatic trapping potential used in each case is shown in the inset.

It is clear that different forms of electrostatic trapping configuration lead to different charge balances. We hope to make a systematic study of this phenomenon in the future and use it to optimize the abundance of particular charge-states. Of the two potential distributions used at present, the square-shaped distribution gives rise to the simpler spectrum and hence is probably more useful in selecting a particular charge state of trapped ions. It is possible however that the inverted bell-shaped distribution is useful for enhancing the population of open-shell ions.

## §4. Conclusion

Clearly, the new EBIT promises many new experiments, with access for spectroscopy from the visible to X-ray energies for a wide range of ionic species. Furthermore, the new trap structure gives extra flexibility in the electrostatic configuration and in the possibility of inducing and observing ion motion, to select and diagnose the relative abundances of charge-states present. It will be possible to perform several different experiments synchronously, maximizing the use of beam time.

## Acknowledgements

The authors are grateful for the Grant-in-Aid for Scientific Research on the priority area, "Atomic Physics of Highly Charged Ions." from the Ministry of Education, Science and Culture. We also thank Sumitomo Heavy Industries Accelerator Division for help in the design and for constructing the EBIT, Yasunori Yamazaki and Ichiro Katayama for the loan of Solid State detectors and Ann Currell for critical reading of this manuscript.

1) M. A. Levine, R. E. Marrs, J. R. Henderson, D. A. Knapp and M. B. Schneider: Phys. Scr. T **22** (1988) 157.
2) E. D. Donets and V. P. Ovsyannikov: Sov. Phys. -JETP **53** (1981) 466.
3) J. D. Silver, A. J. Varney, H. S. Margolis, P. G. E. Baird, I. P. Grant, P. D. Groves, W. A. Hallet, A. T. Handford, P. J. Hirst, A. R. Holmes, D. J. H. Howie, R. A. Hunt, K. A. Nobbs, M. Roberts, W. Studholme, J. S. Wark, M. T. Williams, M. A. Levine, D. D. Dietrich, W. G. Graham, I. D. Williams, R. O'Neil and S. J. Rose: Rev. Sci. Instrum. **65** (1994) 1072.
4) C. A. Morgan, F. G. Serpa, E. Takacs, E. S. Meyer, J. D. Gillaspy, J. Sugar, J. R. Roberts, C. M. Brown and U. Feldman: Phys. Rev. Lett. **74** (1995) 1716.
5) F. J. Currell, J. Asada, K. Ishii, K. Motohashi, N. Nakamura, K. Nishizawa, S. Ohtani, K. Okazaki, M. Sakurai, S. Tsurubuchi and H. Watanabe: *Proc. XIX ICPEAC, Vol. 2, 1995*, p. 792.
6) D. Knapp: NATO ASI Series, *Physics with Multiply Charged Ions.*, ed. D. Liesen, ISBN 0-306-45114-X (1994) p. 143.
7) P. Beiersdorfer, R. E. Marrs, J. R. Henderson, D. A. Knapp, M. A. Levine, D. B. Platt, M. B. Schneider, D. A. Vogel and K. L. Wong: Rev. Sci. Instrum **61** (1990) 2338.
8) D. A. Knapp, R. E. Marrs, C. L. Bennet, M. H. Chen, J. R. Henderson, M. B. Schneider and J. H. Schofiled: Phys. Rev. Lett. **62** (1989) 2104.
9) R. E. Marrs, M. A. Levine, D. A. Knapp and J. R. Henderson: Phys. Rev. Lett. **60** (1988) 1715.
10) P. Beiersdorfer, A. L. Osterheld, M. H. Chen, J. R. Henderson, D. A. Knapp, M. A. Levine, R. E. Marrs, K. J. Reed, M. B. Schneider and D. A. Vogel: Phys. Rev. Lett. **65** (1990) 1995.
11) K. L. Wong, P. Beiersdorfer, D. Vogel, R. Marrs and M.

Levine: Z. Phys. D **21** (1991) S197.
12) D. Schneider, M. A. Briere, J. McDonald and W. Siekhaus: Nucl. Instrum. Methods B **87** (1994) 156.
13) G. Schiwietz, M. Briere, D. Schneider, J. McDonald and C. Cunningham: Nucl. Instrum. Methods B **100** (1995) 47.
14) J. Steiger, G. Weinberg, B. Beck, D. A. Church, J. McDonald and D. Schneider: Nucl. Instrum. Methods B **98** (1995) 569.
15) D. A. Knapp, R. E. Marrs, S. R. Elliot, E. W. Magee and R. Zasadzinski: Nucl. Instrum. Methods A **334** (1993) 305.
16) R. E. Marrs, S. R. Elliot and D. A. Knapp: Phys. Rev. Lett. **72** (1994) 4082.
17) S. R. Elliot and R. E. Marrs: Nucl. Instrum. Methods B **100** (1995) 529.
18) S. R. Elliot: Nucl. Instrum. Methods B **98** (1995) 114.
19) S. R. Elliot, B. Beck, P. Beiersdorfer, D. Church, D. DeWitt, D. K Knapp, R. E. Marrs, D. Schneider and L. Schweikhard: Hyperfine Interact. **81** (1993) 151.
20) R. E. Marrs, P. Beiersdorfer and D. Schnieder: Phys. Today (1994) 27.
21) B. M. Penetrante, J. N. Bardsley, M. A. Levine, D. A. Knapp and R. E. Marrs: Phys. Rev. A **43** (1991) 4873.
22) B. M. Penetrante, J. N. Bardsley, D. DeWitt, M. Clark and D. Schneider: Phys. Rev. A **43** (1991) 4861.
23) K. Watanabe, M. Mizuno, Y. Ohara, M. Tanaka, K. Kobayashi and E. Takahasi: J. Appl. Phys. **72** (1992) 3949.
24) L. S. Brown and G. Gabrielse: Rev. Mod. Phys. **58** (1986) 233.
25) P. Beiersdorfer, St. Becker, B. Beck, S. Elliot, K. Widmann and L. Schweikhard: Nucl. Instrum. Methods B **98** (1995) 558.
26) *Lehrgranshandbuch Kryotechnik*, (Berlin, 1977) vom 3 bis 7.
27) F. J. Currell, J. Asada, K. Ishii, K. Motohashi, N. Nakamura, K. Nishizawa, S. Ohtani, K. Okazaki, M. Sakurai, S. Tsurubuchi and H. Watanabe: *Proc. XIX ICPEAC, Vol. 2, 1995*, p. 798.
28) M. A. Levine, R. E. Marrs, J. N. Bardsley, P. Beirsdorfer, C. L. Bennet, M. H. Chen, T. Cowan, D. Dietrich, J. R. Henderson, D. A. Knapp, A. Osterheld, B. M. Penetrante, M. B. Schneider and J. H. Scofield: Nucl. Instrum. Methods B **43** (1989) 431.
29) G. J. Hermann: Appl. Phys. **29** (1958) 127.
30) POISSON Reference Manual (Los Alamos National Laboratory, 1987) LA-UR-87-126.
31) W. B. Hermannsfeldt: EGUN An Electron Optics and Gun Design Program (Stanford Linear Accelerator Center, 1988) SLAC-Report-331.
32) P. Beiersdorfer, S. von Goeler, M. Bitter, E. Hinnov, R. Bell, S. Bernabei, J. Felt, K. W. Hill, R. Hulse, J. Stevens, S. Suckewer, J. Timberlake, A. Wouters, M. H. Chen, J. H. Schofield, D. D. Dietrich, M. Gerassimenko, E. Silver, R. S. Walling and P. L. Hagelstein: Phys. Rev. A **37** (1988) 4153.